IOPscience iopscience.iop.org

Home Search Collections Journals About Contact us My IOPscience

Extended DFT + *U* + *V* method with on-site and inter-site electronic interactions

This article has been downloaded from IOPscience. Please scroll down to see the full text article.

2010 J. Phys.: Condens. Matter 22 055602

(http://iopscience.iop.org/0953-8984/22/5/055602)

View the table of contents for this issue, or go to the journal homepage for more

Download details:
IP Address: 129.252.86.83
The article was downloaded on 30/05/2010 at 07:02

Please note that terms and conditions apply.

J. Phys.: Condens. Matter **22** (2010) 055602 (12pp) doi:10.1088/0953-8984/22/5/055602

Extended DFT + U + V method with on-site and inter-site electronic interactions

Vivaldo Leiria Campo Jr[1] **and Matteo Cococcioni**[2]

[1] Departamento de Física, Universidade Federal de São Carlos, 13590-905, São Carlos, SP, Brazil
[2] Department of Chemical Engineering and Materials Science, University of Minnesota, Minneapolis, MN 55455, USA

E-mail: vivaldo.leiria@gmail.com

Received 8 October 2009, in final form 9 December 2009
Published 19 January 2010
Online at stacks.iop.org/JPhysCM/22/055602

Abstract
In this paper we introduce a generalization of the popular DFT + U method based on the extended Hubbard model that includes on-site and inter-site electronic interactions. The novel corrective Hamiltonian is designed to study systems for which electrons are not completely localized on atomic states (according to the general scheme of Mott localization) and hybridization between orbitals from different sites plays an important role. The application of the extended functional to archetypal Mott-charge-transfer (NiO) and covalently bonded insulators (Si and GaAs) demonstrates its accuracy and versatility and the possibility to obtain a unifying and equally accurate description for a broad range of very diverse systems.

(Some figures in this article are in colour only in the electronic version)

1. Introduction

Due to its moderate computational cost, the simplicity of its formulation, and the ability to capture the effects of static correlation, the DFT + U method [1, 2] (by DFT + U we generically indicate the Hubbard-corrected local density approximation, LDA + U, or the generalized gradient approximation, GGA + U) has become quite popular in recent years to study systems with strongly localized (typically d or f) and thus, correlated, valence electrons. DFT + U consists of a simple corrective Hamiltonian, added to the (approximate) DFT energy functional, that is shaped on the Hubbard model [3–8]. In its single-band formulation the Hubbard Hamiltonian can be written as follows:

$$H_{\mathrm{Hub}} = t \sum_{\langle i,j\rangle,\sigma} (c^{\dagger}_{i,\sigma} c_{j,\sigma} + \mathrm{h.c.}) + U \sum_{i} n_{i,\uparrow} n_{i,\downarrow} \qquad (1)$$

where $\langle i, j\rangle$ denotes nearest-neighbor sites, $c^{\dagger}_{i,\sigma}$, $c_{j,\sigma}$, and $n_{i,\sigma}$ are electronic creation, annihilation and number operators for electrons of spin σ on site i. The Hubbard model is normally used to describe the behavior of systems in the limit of strong electronic localization. In these conditions the motion of electrons is described by a 'hopping' process from one atomic site to its neighbors (first term of equation (1)), the amplitude of which t is proportional to the bandwidth of the system and thus represents the single-particle term of the total energy. The Coulomb repulsion, instead, is only accounted for between electrons on the same atom through a term proportional to the product of the occupation numbers of atomic states on the same site. The effective strength of the 'on-site' Coulomb repulsion is U. The explicit account for on-site electronic repulsions is ideally suited to study Mott insulators. In fact, in these systems the insulating character of the ground state stems from the dominance of short-range Coulomb interactions (the energy cost of double occupancy of the same site) over single-particle terms of the energy (generally minimized by electronic delocalization) [9] that leads to the localization of electrons on atomic orbitals.

When electrons are strongly localized their motion becomes 'correlated' and their wavefunction acquires a marked many-body character. Capturing all the features of a strongly correlated ground state using effective electronic interaction potentials constructed as functionals of the charge density is a formidable task. In fact, most of the current approximations to the exact DFT energy functional are quite inaccurate in the

 © 2010 IOP Publishing Ltd Printed in the UK

description of the properties of systems characterized by strong electronic localization. In spite of its simplicity, the Hubbard-rooted DFT+U approach has been very effective in alleviating these well known difficulties and has been successfully applied to the study of a large number of quite diverse systems. In recent years it has also been used as the starting approximation for more sophisticated computational methods as, for example, the dynamical mean-field theory (DFT + DMFT) [10, 11] and, more recently, the GW approximation [12, 13].

The 'on-site' Hubbard Hamiltonian contains all the essential ingredients to capture the physics of Mott localization in strongly correlated systems and, in fact, a good description of these systems is usually obtained with DFT + U. A generalized ('extended') formulation of the Hubbard model, with Coulomb interaction terms between electrons on neighbor sites, has been considered since the early days of the Hubbard Hamiltonian [6, 7]. However, to the best of our knowledge, the extended Hubbard model has never been implemented in any DFT-based functional, nor used in *ab initio* calculations. In [14] the authors have stressed the need to consider the off-site interactions and used constrained DFT to evaluate the strength of the on-site U and the inter-site V effective interactions. However, due to its very small value, the inter-site coupling was only used to renormalize the on-site U and all their calculations were performed using the 'standard' DFT + U approach. A simplified formulation of the original extended Hamiltonian (with only charge interactions between pairs of sites) is given in the following expression:

$$H_{\mathrm{Hub}} = t \sum_{\langle i,j\rangle,\sigma} (c^{\dagger}_{i,\sigma} c_{j,\sigma} + \mathrm{h.c.}) + U \sum_{i} n_{i,\uparrow} n_{i,\downarrow} + V \sum_{\langle i,j\rangle} n_i n_j \qquad (2)$$

where V represents the strength of the interaction between electrons on neighbor sites i and j.

The use of the extended model has been stimulated in recent decades by the discovery of high T_c superconductors and the intense research activity focusing around them. Whether the inter-site coupling V has a determinant role in inducing superconductivity is still matter of debate. The 'resonating valence bond' model [15] predicts a superconducting state (at least within mean-field theory) for a doped Mott insulator with only on-site couplings [16]. However, several numerical studies suggest that the inter-site interaction indeed plays an important role [17, 18] and superconductivity is predicted in a regime with repulsive on-site ($U > 0$) and attractive inter-site ($V < 0$) couplings [19–22]. Several studies have also demonstrated that in the 'normal' (non-superconducting) state of superconductors and, in general, in correlated materials, the relative strength of U and V controls many properties of the ground state as, for example, the occurrence of possible phase separations [23], the magnetic order [24, 25], the onset of charge-density and spin-density-wave regimes [26]. In [2, 14] the inter-site coupling (between d states) was recognized to be important in determining a charge-ordered ground state in mixed-valence systems; for Fe_3O_4, however, the computed V was found to be quite small and the authors argued it only contributes an effective renormalization of the on-site U. In [27] the authors used the extended Hubbard model for calculating the Green function of two particles on a lattice and showed that a finite inter-site interaction significantly improves the Auger core–valence–valence line shapes of solids. More recently, the extended Hubbard model has been used to study the conduction and the structural properties of polymers and carbon nano-structures, and the interplay between U and V was shown to control, for example, the dimerization of graphene nanoribbons [28]. The importance of a more accurate account of inter-site couplings, and of the detailed balance with on-site interactions, has also been recognized in a theoretical study of Fe impurities deposited on various alkali metal films [29]. In this case, however, the hybridization between the impurity d states and the s and p orbitals of the alkali metal substrate was described using a one-body term in the Hamiltonian (effectively corresponding to a generalized hopping process between the localized and the delocalized states) rather than a two-body inter-site electronic interaction.

In this work we introduce the extended Hubbard model in DFT-based calculations through a generalization of the DFT + U corrective functional that includes both on-site and inter-site electronic interactions. The main aim of the novel formulation is to improve the accuracy of the DFT+U scheme and to make it quantitatively predictive for systems where the correlation is not strong enough to induce a complete Mott localization of electrons on atomic states, or for which, in general, the hybridization between orbitals belonging to different atoms plays an important role in determining the properties of the ground state. The novel functional is tested on quite diverse bulk solids such as NiO, Si and GaAs. In NiO, a prototype strongly correlated material, d states are quite well localized around Ni atoms. Nevertheless their hybridization with O p states plays a quite significant role and is one of the main factors to determine the charge-transfer insulating character of the material. Si and GaAs are, on the opposite extreme, typical band insulators. The hybridization between s and p orbitals belonging to the same and to neighbor sites plays a dominant role in determining the electronic structure of these materials, as it leads to the formation of bonds in between atoms (with tetrahedral symmetry) and to the consequent onset of the semiconducting character of these systems due to the splitting between bonding (valence) and anti-bonding (conduction) states. The choice of these systems is not casual: a computational scheme that is able to describe accurately strongly localized as well as 'strongly hybridized' systems is likely to be successful for intermediate situations, which are, by far, the most difficult to treat. For each of these test systems we study electronic and structural properties, comparing the results from the new functional with those obtained from 'standard' DFT (GGA) and DFT + U calculations. Improvements obtained with the novel formulation and still remaining issues will be highlighted in each case.

The paper is organized as follows: in section 2 the extended DFT + U + V energy functional is introduced and discussed. In section 3 we present the results obtained from the application of this novel approach to the study of bulk NiO, Si and GaAs. Finally, some concluding remarks are proposed.

2. The extended DFT + U + V functional

The DFT + U approach was formulated and developed in the 1990s [1, 2] to improve the accuracy of (approximate) DFT in describing systems characterized by localized, strongly correlated valence electrons. This scheme is based on a correction to the DFT energy functional that can be generally written as follows:

$$E_{\mathrm{DFT}+U} = E_{\mathrm{DFT}} + E_U = E_{\mathrm{DFT}} + E_{\mathrm{Hub}} - E_{\mathrm{dc}}. \tag{3}$$

In this equation E_{Hub} is the part that contains electron–electron interactions as modeled in the Hubbard Hamiltonian. E_{dc} is a mean-field approximation to E_{Hub} and models the amount of electronic correlation already contained in E_{DFT}. This term is subtracted from the total functional to avoid double counting of the electronic interactions contained in E_{Hub}.

In a commonly used simplified formulation [30] of the rotationally invariant DFT + U [31], to which we will refer in the present work, the total corrective functional has the following expression:

$$E_U = E_{\mathrm{Hub}} - E_{\mathrm{dc}} = \sum_{I,\sigma} \frac{U^I}{2} \mathrm{Tr}[\mathbf{n}^{I\sigma}(\mathbf{1} - \mathbf{n}^{I\sigma})]. \tag{4}$$

In this equation the trace operator indicates the sum over the diagonal elements of the matrix it acts on: $\mathrm{Tr}\{\mathcal{O}\} = \sum_m \mathcal{O}_{m,m}$. $\mathbf{n}^{I,\sigma}$ is the 'on-site' occupation matrix that is defined by the projection of the occupied Kohn–Sham orbitals of spin σ on the localized (atomic) states of orbital quantum number l (typically of d or f kind) ϕ^I_m:

$$n^{I\sigma}_{m,m'} = \sum_{k,v} f^{\sigma}_{kv} \langle \psi^{\sigma}_{kv} | \phi^I_{m'} \rangle \langle \phi^I_m | \psi^{\sigma}_{kv} \rangle. \tag{5}$$

In equation (5) m is the magnetic quantum number associated with l ($-l \leqslant m \leqslant l$), while f^{σ}_{kv} are the occupations of the Kohn–Sham orbitals ψ^{σ}_{kv} based on the distribution of their energies around the Fermi level.

It is useful to show that the functional E_U in equation (4) can be obtained from a mean-field approximation of the electronic interaction energy expressed in terms of atomic orbitals:

$$E_{\mathrm{int}} = \tfrac{1}{2} \sum_{I,J,K,L} \sum_{i,j,k,l} \sum_{\sigma,\sigma'} \langle \phi^I_i \phi^J_j | V_{\mathrm{ee}} | \phi^K_k \phi^L_l \rangle \times \left(n^{KI\sigma}_{k,i} n^{LJ\sigma'}_{l,j} - \delta_{\sigma\sigma'} n^{KJ\sigma}_{kj} n^{LI\sigma'}_{li} \right). \tag{6}$$

In this equation the atomic orbitals are classified by a site index (upper case letter) and a comprehensive state index (lower case letter) that runs over specific manifolds of states of the atom labeled with the same letter (e.g., i indicates atomic orbitals of the atom I). The quantities $\langle \phi^I_i \phi^J_j | V_{\mathrm{ee}} | \phi^K_k \phi^L_l \rangle$ represent the effective Coulomb interactions between the indicated atomic orbitals and $n^{KI\sigma}_{k,i}$ are the mean-field occupation numbers (formally, mean-field averages of creation and annihilation operators, $\langle {c^{I\sigma}_i}^{\dagger} c^{K\sigma}_k \rangle$, to be associated to occupations defined as in equation (5)). The on-site E_{Hub} term of the corrective functional in equation (4) can be formally obtained from the expression in equation (6) neglecting all the interactions but the Hartree and Fock couplings between orbitals on the same site. Due to the localization of atomic states, it is further assumed that the effective interactions are all equal to their atomic averages: $\langle \phi^I_i \phi^J_j | V_{\mathrm{ee}} | \phi^K_k \phi^L_l \rangle \rightarrow \delta_{IK}\delta_{JL}\delta_{IJ}\delta_{ik}\delta_{jl} U^I = \frac{\delta_{IK}\delta_{JL}\delta_{IJ}\delta_{ik}\delta_{jl}}{(2l_I+1)^2} \sum_{i',i''} \langle \phi^I_{i'} \phi^I_{i''} | V_{\mathrm{ee}} | \phi^I_{i'} \phi^I_{i''} \rangle$. Within this approximation one easily obtains:

$$E_{\mathrm{Hub}} = \sum_I \frac{U^I}{2} \left[(n^I)^2 - \sum_{\sigma} \mathrm{Tr}[(\mathbf{n}^{I\sigma})^2] \right] \tag{7}$$

where n^I is the total number of electrons on the atomic states of atom I: $n^I = \sum_{\sigma} \mathrm{Tr}\{\mathbf{n}^{I\sigma}\}$.

The corrective functional in equation (4) was constructed within the so-called 'fully localized limit' (FLL) [32, 33], according to which the double-counting term is the mean-field approximation of E_{Hub} (equation (7)) in the limit where atomic orbitals are either fully occupied or empty. This double-counting functional has the following expression:

$$E_{\mathrm{dc}} = \sum_I \frac{U^I}{2} n^I (n^I - 1). \tag{8}$$

Subtracting equation (8) from (7), E_U in equation (4) is exactly reproduced.

Generalizing the approach described above, the E_{Hub} of DFT + U + V can be obtained from equation (6) supposing that a significant contribution to the corrective potential also comes from the interactions between orbitals on pairs of distinct sites. Similarly to the on-site case, the (Hartree–Fock-like) effective inter-site interactions are all assumed to be equal to their atomic averages over the states of the two atoms: $\langle \phi^I_i \phi^J_j | V_{\mathrm{ee}} | \phi^K_k \phi^L_l \rangle \rightarrow \delta_{IK}\delta_{JL}\delta_{ik}\delta_{jl} V^{IJ} = \frac{\delta_{IK}\delta_{JL}\delta_{ik}\delta_{jl}}{(2l_I+1)(2l_J+1)} \sum_{i',j'} \langle \phi^I_{i'} \phi^J_{j'} | V_{\mathrm{ee}} | \phi^I_{i'} \phi^J_{j'} \rangle$. Note that $V^{II} = U^I$. Within this hypothesis it is easy to derive the following expression:

$$E_{\mathrm{Hub}} = \sum_I \frac{U^I}{2} \left[(n^I)^2 - \sum_{\sigma} \mathrm{Tr}[(\mathbf{n}^{II\sigma})^2] \right] + \sum_{IJ}^{\star} \frac{V^{IJ}}{2} \left[n^I n^J - \sum_{\sigma} \mathrm{Tr}(\mathbf{n}^{IJ\sigma} \mathbf{n}^{JI\sigma}) \right] \tag{9}$$

where the star in the sum operator denotes that for each atom I, index J covers all its neighbors up to a given distance (or belonging to a given shell). Equation (9) uses a generalized formulation of the occupation matrix (equation (5)) to allow for the possibility that the two atomic wavefunctions involved in its definition belong to different atoms:

$$n^{IJ\sigma}_{m,m'} = \sum_{k,v} f^{\sigma}_{kv} \langle \psi^{\sigma}_{kv} | \phi^J_{m'} \rangle \langle \phi^I_m | \psi^{\sigma}_{kv} \rangle. \tag{10}$$

In equation (10) the indexes m and m' run over the angular momentum manifolds that are subjected to the Hubbard correction on atoms I and J respectively. It is important to notice that the occupation matrix defined in equation (10) contains information about all the atoms in the same unit cell and the on-site occupations defined in equation (5) correspond to its diagonal blocks ($\mathbf{n}^{I\sigma} = \mathbf{n}^{II\sigma}$).

For a complete expression of the DFT + U + V corrective functional, a double-counting term needs to be defined as well. Generalizing the FLL expression of the on-site double-counting term, we arrive at the following expression:

$$E_{\rm dc} = \sum_I \frac{U^I}{2} n^I (n^I - 1) + \sum_{I,J}^{\star} \frac{V^{IJ}}{2} n^I n^J. \qquad (11)$$

Subtracting equation (11) from (9) we finally obtain:

$$E_{UV} = E_{\rm Hub} - E_{\rm dc} = \sum_{I,\sigma} \frac{U^I}{2} {\rm Tr}[\mathbf{n}^{II\sigma}(\mathbf{1} - \mathbf{n}^{II\sigma})] - \sum_{I,J,\sigma}^{*} \frac{V^{IJ}}{2} {\rm Tr}[\mathbf{n}^{IJ\sigma}\mathbf{n}^{JI\sigma}]. \qquad (12)$$

Having neglected the orbital dependence of the effective coupling parameters (equation (6)) and all the interaction terms involving states that belong to three and four distinct atomic sites, the corrective functional in equation (12) necessarily corresponds to a quite drastic approximation of the full many-body part of the electronic Hamiltonian. To discuss the underlying approximations in some detail it is convenient to introduce the following notation: $A^{IJKL}_{ijkl} = \langle \phi^I_i \phi^J_j | V_{\rm ee} | \phi^K_k \phi^L_l \rangle (n^{KI,\sigma}_{ki} n^{LJ,\sigma'}_{lj} - \delta_{\sigma\sigma'} n^{KJ,\sigma}_{kj} n^{LI,\sigma'}_{li})$. It is easy to see that the inter-site interaction included in the DFT + U + V functional defined in equation (12) corresponds to the terms A^{IJIJ}_{ijij} (with electronic couplings averaged over the orbitals of the two sites). Other contributions describing cross charge exchanges between neighbor sites (A^{IJJI}_{ijji}), double (parallel) electron transfers from one site to a neighbor one (A^{IIJJ}_{iijj}), couplings between on-site charge and hopping from/to the same site $A^{IIIJ}_{ii'ij'}$, and coupled intra-site charge exchanges (as, e.g., $A^{IJIJ}_{iji'j'}$) are all neglected. The terms included in our corrective functional, A^{IJIJ}_{ijij}, correspond to the sum of the (atomically averaged) Hartree interactions between the charge densities of two atomic states (either on the same site or on distinct ones) and the corresponding exchange counterparts. Due to the localization of the atomic orbitals and the orthonormality condition imposed between them, these terms are probably the dominant ones from a numerical point of view. However, because of cancelation between $E_{\rm Hub}$ and $E_{\rm dc}$ only the exchange terms survive in the final expression of E_{UV} (equation (12)), both in the on-site and in the inter-site parts. The choice of these terms is indeed consistent with the approximation used in the original formulation of the extended Hubbard model [6, 7] and in quite abundant literature where the inter-site interaction is usually included through a $V^{IJ} n^I n^J$ term.

As evident from equation (4), the on-site term of the total energy introduces a finite energy cost for fractional atomic occupations (if $\lambda^{I,\sigma}_m$ is one eigenvalue of $n^{II\sigma}$, E_U is 0 for $\lambda^I_m = 0$ or 1, positive otherwise); this penalty favors a Mott-like ground state with correlated electrons localized on atomic orbitals. The effect of the inter-site interaction can be easily understood from the contribution of the corrective functional in equation (12) to the total Kohn–Sham potential. This quantity can be computed as the functional derivative of the energy with respect to $(\psi^\sigma_{kv})^*$:

$$V_{UV}|\psi^\sigma_{kv}\rangle = \frac{\delta E_{\rm Hub}}{\delta (\psi^\sigma_{kv})^*} = \sum_I \frac{U^I}{2} \sum_{m,m'} (\delta_{mm'} - 2n^{II\sigma}_{m'm}) |\phi^I_m\rangle \langle \phi^I_{m'} | \psi^\sigma_{kv}\rangle - \sum_{I,J}^{*} V^{IJ} \sum_{m,m'} n^{JI\sigma}_{m'm} |\phi^I_m\rangle \langle \phi^J_{m'} | \psi^\sigma_{kv}\rangle. \qquad (13)$$

From equation (13) it is evident that the *on-site* term of the potential is attractive for occupied states that are, at most, linear combinations of atomic orbitals of the *same atom* (resulting in on-site blocks of the occupation matrix, $\mathbf{n}^{II\sigma}$, dominant on others), whereas the *inter-site* one stabilizes states that are linear combinations of atomic orbitals belonging to *different atoms* (e.g., molecular orbitals, that lead to large off-site blocks, $\mathbf{n}^{JI\sigma}$, of the occupation matrix). Thus, a competition sets in between two opposite tendencies that allows for more general localization regimes and increases the coupling between orbitals on different sites. Obviously, the character of the electronic ground state depends critically on the relative strength of the on-site (U) and the inter-site (V) electronic interactions. The detailed balance between these quantities is guaranteed by the possibility of computing both parameters simultaneously through the linear-response approach described in [34]. In fact, the inter-site interaction parameters correspond to the off-diagonal terms of the interaction matrix defined in equation (19) of [34].

It is important to notice that the trace operator in the on-site functional guarantees the invariance of the energy only with respect to rotations of atomic orbitals *on the same atomic site*. In fact, the on-site corrective functional (equation (7)) is not invariant for general rotations of the atomic orbital basis set mixing states from different atoms. In the inter-site term (equation (12)), the trace applied to the product of generalized occupation matrices is not sufficient to re-establish this invariance. In fact, for the corrective functional to be invariant, the elements of the electronic interaction matrix should transform as quadruplets of atomic orbitals and thus have full site and orbital dependence. As discussed above, instead, at the present level of approximation, interactions between more than two atomic sites are assumed to be less important than the ones included in equation (12) and orbital dependence is totally neglected. Nonetheless, the inter-site extension of the corrective functional represents, with respect to the on-site case, a significant step towards general invariance, as it contains, at least, some of the multiple-site terms that would be generated by the rotation of on-site ones. Furthermore, the possibility of evaluating both U and V from linear-response theory [34] (at least for interactions between pairs of atomic sites), guarantees a high level of consistency between the atomic orbital basis set and the interaction parameters used in the functional, and reduces the dependence of the results on the specific choice of the localized basis. Site and orbital dependence of the corrective functional are implicitly included in Wannier-function-based implementations of DFT + U [35–37], as becomes evident by re-expressing Wannier functions on the basis of atomic

orbitals. The two approaches would thus lead to equivalent results if all the relevant multiple-center interaction parameters are included in the corrective functionals and are computed consistently with the choice of the orbital basis. While on the basis of Wannier functions the number of relevant electronic interactions to be computed is probably minimal (especially if maximally localized orbitals are considered [38]), the atomic orbital representation, besides providing a more intuitive and transparent scheme to select relevant interaction terms (e.g., based on inter-atomic distances), is more convenient to compute derivatives of the energy as, for example, forces and stresses that are crucial to evaluate the structural properties of systems.

In the implementation of equation (12) we have added the possibility for the corrective functional to act on two l manifolds per atom as, for example, orbitals 3s and 3p in Si, or orbitals 4s and 3d in Ni. To the best of our knowledge, this feature has been implemented only recently in a 'standard' (on-site) DFT + U functional [39] where, however, at variance with our formulation, no interaction was established between the two manifolds of the same atom. If we call 'standard' the higher l states of each atom the Hubbard correction acts on, and 'background' the other l manifold being corrected, for a given pair of atomic sites I and J (equation (12)), we have four interaction parameters: standard–standard, standard–background, background–standard, and background–background. Alternatively, the different Hubbard-corrected manifolds on each atom can be seen as belonging to different atoms located at the same crystallographic site. The motivation for this extension consists in the fact that different manifolds of atomic states may require to be treated on the same theoretical ground in cases where hybridization is relevant (as, e.g., for bulk diamond whose bonding structure is based on the sp^3 mixing of s and p orbitals). The particular choice to have different interaction parameters acting on different manifolds of atomic states, and the possibility to include 'cross-manifold' interactions (basically 'on-site' V parameters between standard and background states) eliminates the need of explicit intervention in the construction of the basis set for cases where localization is expected to occur on states different from atomic orbitals (as, for example, in [40–42]).

While the inter-site interaction V can be calculated at the same time as the on-site U and with no additional cost, the computational workload of a DFT + U + V calculation depends on the number of neighbors between which the inter-site correction is established. For interactions between nearest neighbors (all contained in a $3\times3\times3$ supercell centered around the primitive one) the computational cost is only marginally bigger than for an on-site-only DFT + U; if further shells of neighbors are included in the summation of equation (12), larger supercells around the primitive one may be needed and the search of equivalent neighbors may increase significantly the cost of the calculation (up to a 18% increase in the cpu time for a $5 \times 5 \times 5$ supercell compared to a $3 \times 3 \times 3$ one).

3. Results and discussions

In this section we present the results obtained with the novel functional applied to the study of the selected test systems: NiO, Si, and GaAs. The choice to test a numerical approach which traditionally would be used only for strongly correlated materials on band insulators can appear unusual. From a theoretical point of view, it is important to notice that, in the context of DFT, the fundamental gap of Mott insulators coincides with the discontinuity of the exact exchange–correlation potential with respect to the number of particles, (see, for example [43–45]); at the same time the absence of such a discontinuity in approximate energy functionals often leads to severe underestimates of the energy gap of band insulators and semiconductors [46, 47]. From this point of view, if DFT + U is effective in re-introducing this specific feature in the energy spectrum of a strongly correlated system, there is no reason for this approach not to be as effective for other classes of materials. The only limitation to the use of this approach to a broader class of system could consist in the formulation of the corrective functional not being flexible enough to describe more general localization regimes (in fact, the 'standard' DFT + U was designed to describe correlation-driven localization of electrons on atomic orbitals according to the original Mott picture). This is indeed the aspect we want to investigate through the development and the use of the general DFT + U + V scheme. Analogous considerations to ours have led the authors of [48] to operate a similar selection of systems to test their reduced density matrix functional (RDMF) approach.

For all these systems, comparison will be made with the results obtained with DFT and with the 'standard', on-site DFT + U. All the calculations were performed using the plane-waves pseudopotential 'pwscf' code contained in the *Quantum ESPRESSO* (QE) package [49], where we implemented the '$+U+V$' correction starting from an existing on-site DFT + U functional [49].

It is important to remark that for all the systems treated in this work U and V were obtained using the linear-response approach described in [34]. However, at variance with the calculations presented in [34], the response matrices were not constrained to give a neutral total response (in terms of on-site occupations) when the perturbation is applied on every atom. While this has no effects on the final results if large enough supercells are used in the calculations, we believe it to be a better strategy to compute the effective interactions, especially if the response of all atomic orbitals (standard plus background) is explicitly considered. A further difference with the results presented in [34] consists in the use of orthogonalized atomic orbitals to construct occupation matrices. While not necessary, this choice guarantees that the atomic occupation matrices satisfy more stringent sum rules (their trace represents more closely the total number of electrons on atomic states). Some small differences are to be expected with the results obtained for NiO in [34]; however, we believe that the consistent evaluation of the effective electronic interactions (especially if obtained from a DFT + U ground state) reduces these differences to a minimal value.

3.1. NiO

As other transition metal oxides with the same stoichiometry, nickel oxide has a cubic rock-salt crystalline structure. Below a Neél temperature of 523 K, the magnetic moments of Ni atoms arrange in an antiferromagnetic (AF) order (usually referred to as AFII) where ferromagnetic (111) Ni planes alternate with opposite magnetization. As a consequence of the AF magnetic order the crystal acquires a rhombohedral symmetry. Transition metal oxides (TMOs) have represented a significant challenge for theorists, since their insulating character can not be explained satisfactorily using band theory, due to the intrinsic many-body origin of their band gap. Although within Kohn–Sham (KS) theory the energy spectrum has no precise physical meaning and is not guaranteed to reproduce the band gap of the system, once the finite discontinuity of the (exact) exchange–correlation potential is added to the KS HOMO–LUMO energy difference the correct band gap should be exactly reproduced [43, 45]. Failing to properly incorporate many-body effects, most approximate exchange–correlation functionals produce no discontinuity in the corresponding potentials, thus resulting in quite poor estimates of band gaps or in their total suppression. In fact, many TMOs are predicted to be metallic, in striking contrast with the observed insulating character. In some of these systems (e.g., FeO [34]) a lack of proper accounting of the many-body aspects of the electronic structure also results in serious inaccuracies in the description of the structural and magnetic properties. Similar problems can be expected for NiO even if a gap (still significantly smaller than the experimental one) fortuitously opens in its Kohn–Sham spectrum as the result of the balance between the exchange and the crystal-field splitting among the d states of Ni (nominally occupied by eight electrons). Photoemission experiments on NiO have measured a band gap of about 4.3 eV (3.1 eV at the minimum intensity) [50] and have explored several features of the spectrum assessing, in particular, its charge-transfer character [50–52]. In fact, the excitation of one electron across the band gap of the quasi-particle spectrum corresponds to its transfer from the p states of a ligand oxygen atom to the d states of a Ni atom. As a consequence, the top of the valence band is dominated by the p states of oxygen while the bottom of the conduction one largely consists of Ni d states. Computational studies on this material have been quite successful in reproducing these features of its spectrum. DFT + U, whose corrective potential is designed to introduce a finite energy difference between occupied and unoccupied states, can be expected to produce a more accurate estimate of the fundamental gap of a system (in principle larger than the one appearing in photoemission experiments). In fact, it has been used quite successfully to study NiO and has produced a band gap of about 3.0–3.5 eV (the precise value varies with the U used in different works) and quite accurate estimates for both the magnetic moments and the equilibrium lattice parameter [53–55]. For other details of the density of states (as, e.g., the spectral weight of O p states on top of the valence band), the agreement is not unanimous. DFT + U has also been employed recently to compute the k-edge XAS spectrum of NiO using a novel, parameter-free computational approach [56] that has produced results consistent with experimental data. In this paper the authors highlight the importance of non-local excitation of d states and, specifically, those involving second-nearest-neighbor Ni atoms. The same intent of improving the description of spectroscopic properties has been pursued with the GW approximation based on a DFT + U ground state [12, 13]; this approach has provided a better estimate of the energy gap compared to DFT + U, even though other details of the density of states were almost unchanged [12]. Hartree–Fock (HF) [57] and hybrid functionals (e.g. B3LYP) [57, 58] have also been used to study NiO. While pure HF overestimates the size of the band gap and fails to reproduce its charge-transfer nature, hybrid functionals are more accurate and result in a better estimate of the properties of this material. Most recently DFT + DMFT calculations of NiO have explored the effects of dynamical correlations and have produced a band gap in the energy spectrum in excellent agreement with photoemission experiments, even though its charge-transfer character was not always well reproduced [59, 60]. A modification to this method within the iterative perturbation theory has been recently used to fix this particular aspect of the calculated spectrum of NiO [61]. In this paper, the authors also present a detailed discussion of the features of the DOS, remarking the role of dynamical correlations (e.g., in eliminating the excessive spectral weight of mixed Ni e_g and O p states at the bottom of the valence band, normally observed in DFT + U and GW), and the importance that inter-spin and inter-atomic components of the self-energy would have in fixing some still remaining discrepancies in the computed spectrum compared to the experimental one (e.g., the position of the occupied satellite). This latter hypothesis will be discussed with the results of the present work where inter-atomic couplings are explicitly taken into account thanks to the extended functional introduced in section 2.

All calculations presented in this paper were performed in the AF configuration of the system. We used ultrasoft [62] GGA pseudopotentials constructed with the PBE parametrization [63]. Accurate estimates of the total energies required energy cut-offs of 40 and 400 Ryd for the plane-wave expansion of wavefunctions and charge density respectively and a $4 \times 4 \times 4$ Monkhorst–Pack k-point grid [64] to sample the Brillouin zone of this system.

The electronic interaction parameters (U and V) used in this work were recomputed for each considered lattice spacing (using the linear-response approach of [34]). Figure 1 shows the dependence of some of these parameters on the size of the unit cell. It is important to remark that these parameters are not directly comparable with those evaluated in [34] for two reasons: first, in the present calculations we have explicitly included the response of the 'background' states, which could not be done in the previous work; second, at variance with what was done in [34] to define the on-site occupation matrix we have used atomic orbitals that were preliminarily orthogonalized. However, since Us and Vs are consistently computed and used within the same approximation (i.e., using the same definition of the occupations) in both works, the most significant differences are expected to arise from using a V-augmented functional.

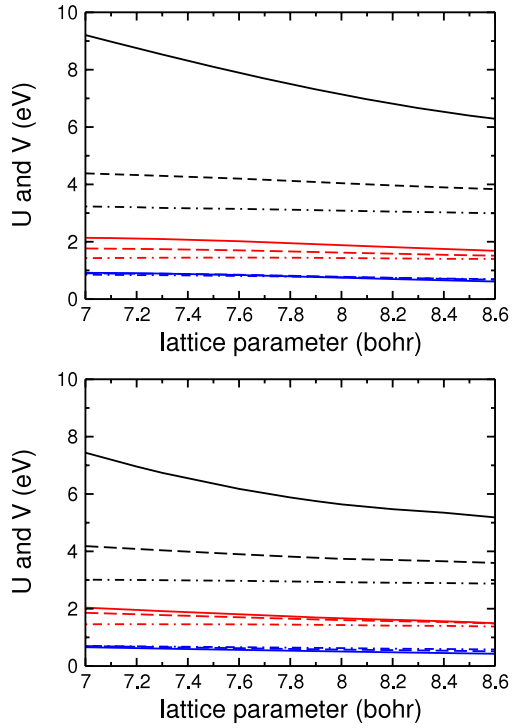

Figure 1. (Color online) The variation of the on-site and inter-site electronic couplings as functions of the cubic lattice parameter of NiO. The interaction parameters were obtained from a GGA ground state (top graph) or from a GGA + U + V ground state (bottom graph) according to a self-consistent procedure (see text). Black lines represent on-site (Ni only) interactions, red ones describe the couplings between nearest neighbors (Ni–O), blue ones between next-nearest neighbors (Ni–Ni). Solid lines are for standard–standard, dashed for standard–background, and dot-dashed for background–background interactions respectively.

As can be observed from figure 1 (top graph) the on-site U is the parameter that changes the most with the size of the unit cell. Other electronic couplings are much less affected and the dependence of the interaction between second-nearest neighbors (Ni–Ni) on the lattice parameter is almost negligible. While the parameters shown in the top graph of figure 1 were obtained from the GGA ground state of the system, those represented in the bottom graph were computed 'self-consistently' from a GGA + U + V ground state using a method equivalent to that of [65], but based on a more efficient algorithm that will be described elsewhere. Although all the electronic interactions are obtained at the same time (including those for 'background' states and their coupling with 'standard' ones) the interaction parameters between the p states and between p and s states of oxygen (all U_{O} and $V_{\mathrm{O-O}}$) were excluded from our DFT + U + V calculations. While a rigorous motivation for this choice is presently missing, we believe that the corrective action of the '+U + V' functional is mostly needed for open manifolds around the Fermi level (or the top of the valence band) while the p and s states of oxygen are almost completely full. Besides the on-site U_{Ni}, first ($V_{\mathrm{Ni-O}}$) and second ($V_{\mathrm{Ni-Ni}}$) nearest-neighbor inter-site couplings (between 'standard' and 'background' states) were all included in our calculations; the inclusion of the interactions between further neighbors was found to produce no relevant effect. For all the approaches compared in this work (GGA, GGA + U and GGA + U + V) the optimization of the rock-salt cubic structure (in the AF ground state) was performed using the cell-size-dependent electronic couplings plotted in figure 1, fitting the dependence of the total energy on its volume on a Murnaghan equation of state. Using size-dependent electronic couplings has been recently shown to be fundamental for quantitative descriptions of the structural and electronic properties of materials and for accurate evaluations of transformation pressures between, e.g., different spin or structural phases [66, 67].

Table 1. The equilibrium lattice parameter, (a, in Bohr atomic radii), the bulk modulus (B, in GPa), and the band gap (E_{g}, in eV) of NiO obtained with different computational approaches: GGA, 'traditional' GGA + U (with U only on the d states of Ni), GGA + U + V and a 'self-consistent' GGA + U + V with the interaction parameters computed from a GGA + U + V ground state (see text). Comparison is made with the experimental results on all the computed quantities.

	a	B	E_{g}
GGA	7.93	188	0.6
GGA + U	8.069	181	3.2
GGA + U + V	8.031	189	3.6
GGA + U + V^{sc}	7.99	197	3.2
Exp	7.89[a]	166–208[b]	3.1–4.3[c]

[a] Reference [68]. [b] Reference [69].
[c] Reference [50, 52].

Table 1 compares the equilibrium lattice parameters, the bulk moduli, and the energy band gap obtained in the three different approaches with results from experiments. In each case the band gap of the material was measured for the equilibrium lattice parameter reported in the same table. A comparison between the DOS obtained within the different approaches is made in figure 2.

Our GGA calculations (figure 2, top graph) result in an equilibrium lattice spacing of 7.93 Bohr, which is quite consistent (+0.5%) with the experimental value of 7.89 Bohr and provides a good estimate of the bulk modulus (187.7 GPa). As expected from other GGA results, the band gap (∼0.6 eV) is smaller than the observed one (3.0–4.3 eV) and its spectroscopic nature is also not consistent with experiments as the top of the valence band is dominated by the d states of Ni instead of O p. It is important to notice that the peak at 5 eV below the edge of the valence band contains contributions from both O and Ni and, as specified in other works (see, e.g., [55]), is the signature of the hybridization between d_{e_g} and p states. This is a spurious feature, as the lowest part of the valence manifold should be dominated by t_{2g} states instead [50–52].

GGA + U (U on Ni d states only) leads to a significant improvement in the size of the band gap (3.2 eV) compared to GGA, and O p states are dominant on the top of the valence band in agreement with experimental results (figure 2, second graph from the top). The equilibrium lattice parameter obtained with GGA + U (8.069 Bohr) is larger than the one obtained with GGA, less in agreement with experiments (table 1). Also, the crystal resulting is softer with a bulk

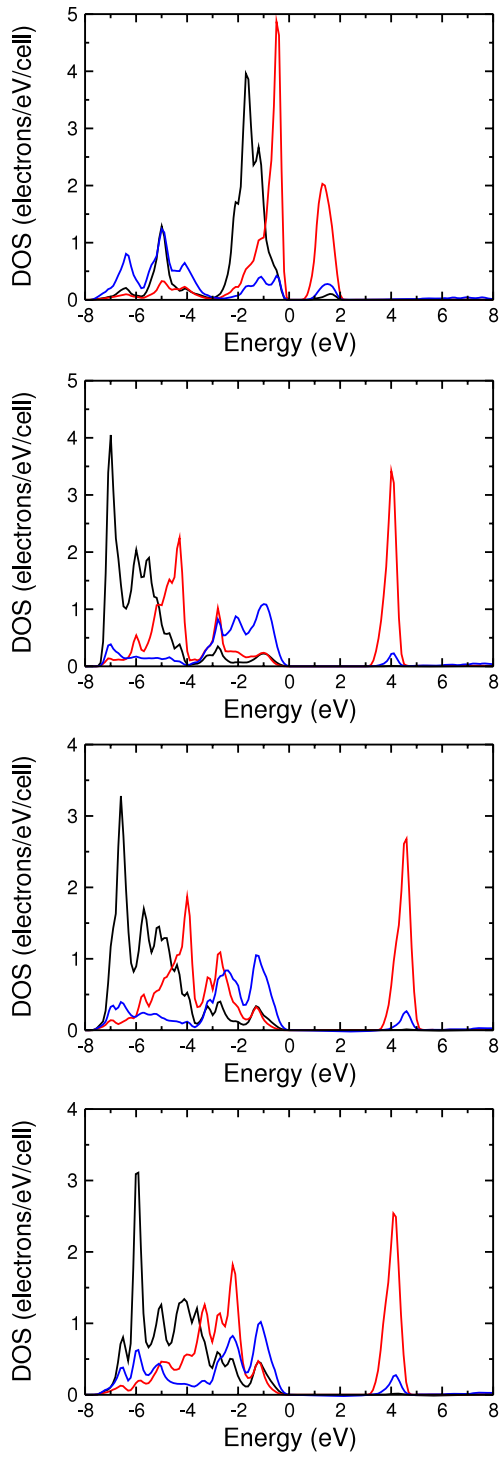

Figure 2. (Color online) The density of states of NiO obtained with different approximations: (a) GGA; (b) GGA + U (U on Ni d states only); (c) GGA + U + V including on-site (U_{Ni}) and inter-site ($V_{\mathrm{Ni-Ni}}$ and $V_{\mathrm{Ni-O}}$) interactions computed from a GGA ground state; (d) GGA + U + V with interactions computed 'self-consistently' from a GGA + U + V ground state. In all graphs the black and red lines represent majority and minority spin d states of Ni, the blue line the p states of O. The energies were shifted for the top of the valence band to correspond to the zero of the energy in all cases.

modulus of about 181 GPa (still in the range of experimental results). While the almost exclusive presence of p bands on top of the valence band seems to overestimate the spectral weight of these states compared with the results of other calculations [53–55], the dominant p character of the peak at −2 eV, and the appearance of a peak at −4.5 eV, mainly due to minority spin t_{2g} Ni states, have not been highlighted in experiments [52]. However, the position of a strong peak in the DOS, at about −7 eV from the valence band edge, appears consistent with experimental results [50], although further analysis would be needed to assess its character. The clear-cut separation between p states and lower energy d states is, instead, unusual for DFT+U calculations. This latter aspect may be due to the different value of the U parameter used with respect to other calculations of this kind.

Using GGA + U + V (figure 2, third graph from the top), the equilibrium lattice parameter (table 1) is corrected towards the experimental value (8.03 Bohr), while the bulk modulus equals 189 GPa and a band gap of about 3.6 eV opens between O p and Ni d states correctly placed at the top of the valence band and the bottom of the conduction one respectively. The band structure of the system shows some differences from the one obtained with GGA+U. With respect to the GGA + U results, the minority spin d states of Ni have moved upwards in energy and show a larger overlap with the p states of O, suggesting a larger degree of hybridization. As a result, the peak at −2.5 eV acquires a markedly mixed d and p character, and the central peak, mainly due to Ni minority spin d states, moves to slightly higher energy at −4 eV from the gap. The occupied satellite peak, which also appears at slightly higher energy (≈−6.5 eV) than in the GGA + U DOS, is still dominated by Ni majority spin d states.

Using the 'self-consistent' GGA + U + V (i.e., with U and V computed from a GGA + U + V ground state) we obtained an equilibrium structure in better agreement with experimental results (a = 7.99 Bohr), a bulk modulus of about 197 GPa (still within the range of available experimental data) and a band gap of 3.2 eV (figure 2, bottom graph). The electronic structure in this case is quite similar to that obtained within the non-self-consistent GGA+U+V approach (figure 2, third graph from top). However an even larger overlap can be observed between Ni d and O p states in the upper part of the spectrum, with a peak below the edge of the valence band at ≈−2.2 eV that is dominated by Ni states, in agreement with experiments [50]. The occupied satellite peak, at about −6 eV, is still dominated by Ni d states, although the p state component seems slightly more significant in this case. It is important to notice that the valence DOS has now acquired three dominant features that correspond to the O peak at the top of the band, a Ni-dominated peak at about −2.2 eV and a strong d peak at −6 eV. These characteristics are consistent with the results from photoemission experiments, although the relative spectral weight of these peaks are not in quantitative agreement with observations. Furthermore we do not observe the downshift of the occupied satellite (actually moved to slightly higher energies) that in [61] is expected to arise from the explicit inclusion of inter-site electronic interactions in the corrective functional. In our opinion these discrepancies are due to the fact that, at the present level of approximation, electronic interaction parameters are only site dependent. While dynamical correlation may

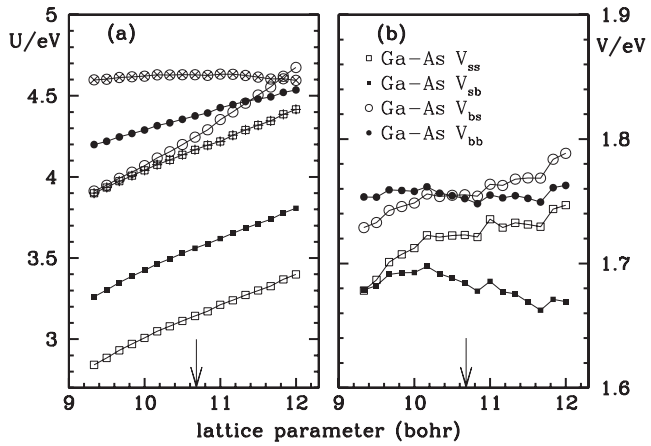

Figure 3. Intra-site (U) and inter-site (V) interaction parameters as functions of lattice parameter for GaAs with 3d electrons as valence electrons. (a) Intra-site interactions. Squares correspond to Ga atoms and circles to As atoms. Open symbols represent U_{ss} (standard–standard), filled symbols represent U_{sb} (standard–background) and symbols with crosses represent U_{bb} (background–background). (b) Inter-site interactions. Arrows indicate the equilibrium lattice parameter.

play an important role, as demonstrated by DFT + DMFT calculations [59–61], we believe that the most significant refinement needed to reproduce all the details of the spectrum of the material consists in the formulation of an extended model with fully orbital-dependent interaction parameters. Specifically, a distinction should be made between the (inter-site) interactions of O p states with Ni t_{2g} and e_g states.

In summary, GGA + U + V offers a quite significant improvement in the description of NiO compared to GGA + U, and we believe that in providing a more realistic representation of electronic and structural properties it can be a better starting approximation for numerical approaches (as GW or DFT + DMFT) aimed at predicting the excitation spectrum of the material or at studying the effects of dynamical correlations.

3.2. Si and GaAs

For Si and GaAs, DFT calculations based on LDA and GGA approximate functionals provide results for the structural properties (e.g., the lattice parameter and the bulk modulus and its first derivative) [70–72] and the vibrational spectrum [73] in good to excellent agreement with experiments. GGA normally results in slightly larger equilibrium lattice constants and softer bulk moduli than the measured ones [71, 72, 74]. However, for reasons mentioned in one of the previous sections, the computed band gap of these materials systematically underestimates the experimental value. Many corrective approaches have been developed to overcome these difficulties inherent to standard DFT approximations, and quite good agreement with the experimental spectrum could be obtained using the exact exchange (EXX) [75, 76], hybrid functionals [77], or methods specifically designed to reproduce the electronic excitation spectrum, such as the GW approach based on an LDA [78, 79]

Table 2. Interaction parameters U and V (eV) for Si and GaAs (Note: Ga 3d electrons as valence electrons.) Inter-site terms are for first neighbors and the listed values are for the equilibrium lattice parameters found with GGA + U + V. Indexes s and b stand for 'standard' and 'background' orbitals respectively, as discussed in the text.

	U_{ss}	U_{sb}	U_{bs}	U_{bb}	V_{ss}	V_{sb}	V_{bs}	V_{bb}
Si–Si	2.82	3.18	3.18	3.65	1.34	1.36	1.36	1.40
Ga–Ga	3.14	3.56	3.56	4.17				
As–As	4.24	4.38	4.38	4.63				
Ga–As					1.72	1.68	1.76	1.75

or a EXX [80] ground state. In the present work, we investigate the performance of the GGA + U + V functional on Si and GaAs and compare its results with those from standard GGA and GGA + U. In these semiconductors, the hybridization between s and p orbitals and the formation of covalent bonds between neighbor atoms are key ingredients to understand their structural and electronic properties. Thus, the corrective functional introduced in the present paper has to contain coupling terms between neighbor atoms and between s and p manifolds on the same site.

As mentioned above, for both Si and GaAs we have used GGA exchange–correlation functionals constructed with the PBE parametrization [63]. In particular for Si we employed a norm-conserving pseudopotential. This potential required an energy cut-off of 40 Ryd for the plane-wave expansion of the Kohn–Sham wavefunctions. For GaAs we used, instead, ultrasoft pseudopotentials [62] that required cut-offs of 40 and 400 Ryd for the expansion of the electronic wavefunctions and charge density respectively. As [81] points out, predictions for gallium compounds can be very sensitive to the inclusion of 3d electrons in the valence manifold for Ga pseudopotentials. Thus, two alternatives were considered, with Ga 3d electrons in the valence manifold or frozen in the core. We will refer to these two different situations as GaAs(v) and GaAs(c) respectively. For both materials (Si and GaAs), the Brillouin zone was sampled with a 8 × 8 × 8 Monkhorst–Pack [64] k-point grid.

In order to determine the equilibrium lattice parameter and the bulk modulus, the dependence of the ground state energy on volume was fitted by the Murnaghan equation of state. As in the case of NiO, DFT + U and DFT + U + V total energy calculations were performed using effective interactions consistently recomputed for each value of the lattice parameter. Figure 3 illustrates the dependence of Us and Vs on the size of the unit cell in the case of GaAs(v). In table 2, the on-site and inter-site interactions computed at the equilibrium lattice parameter are grouped to ease the comparison. It is important to notice that the values of either the Us or the Vs are very similar, irrespective of the orbital manifold they act on (p or s states). This result, more evident for GaAs and for the inter-site couplings, is due to the hybridization of p and s orbitals and corroborates the need to treat both types of states at the same level.

In table 3, the equilibrium lattice parameter, the bulk modulus and the band energy gap obtained from GGA, GGA + U and GGA + U + V calculations on Si and GaAs can

Table 3. Comparative results for lattice parameter (a, in Å), bulk modulus (B, in GPa) and energy gap (E_g, in eV).

	Si			GaAs(v)[a]			GaAs(c)[b]		
	a	B	E_g	a	B	E_g	a	B	E_g
GGA	5.479	83.0	0.64	5.774	58.4	0.19	5.578	65.7	1.25
$+U$	5.363	93.9	0.39	5.736	52.6	0.00	5.616	62.7	0.81
$+U+V$	5.370	102.5	1.36	5.654	67.7	0.90	5.535	76.5	1.97
Exp.[c]	5.431	98.0	1.12	5.653	75.3	1.42	5.653	75.3	1.42

[a] Ga 3d electrons as valence electrons.

[b] Ga 3d electrons in the core.

[c] At 300 K, from [82]. At 0 K, the energy gaps of Si and GaAs are estimated to be 1.17 eV and 1.52 eV respectively [82].

be directly compared with experimental measurements of the same quantities (we refer to the data collected in the web database, [82]). As expected from abundant literature, GGA overestimates the equilibrium lattice parameter with respect to the experimental value (except for the case of GaAs(c)), while the bulk modulus and the band gap are underestimated in all cases. On-site GGA + U predicts the equilibrium lattice parameter in better agreement with the experimental value (overcorrected for Si); however, the bulk modulus is improved with respect to the GGA value only in the case of Si. In all three cases, however, the energy band gap is lowered compared to GGA, further worsening the agreement with experiments. While this result may appear strange, it is not unexpected. In fact the on-site corrective functional suppresses the hybridization between states on neighbor atoms that is largely responsible for the band gap in semiconductors between valence (bonding) and conduction (anti-bonding) states. The use of the inter-site correction, in spite of the fact that Vs are smaller than half the on-site Us, results in a systematic improvement for the evaluation of all these quantities. In fact, encouraging the occupations of hybrid states, the inter-site interactions not only enlarge the splitting between populated and empty orbitals (which increases the size of the band gap), but also make the bonds shorter (so that hybridization is enhanced) and stronger, thus tuning both the equilibrium lattice parameter and the bulk modulus of these materials to values closer to experimental results. For GaAs, the calculations with the Ga 3d states in valence are more accurate than the ones with these atomic states frozen in the core. In fact, for GaAs(v) we obtain an equilibrium lattice parameter in excellent agreement with the measured one. The bulk modulus and the band gap, while smaller than the experimental values, are significantly closer to these than the estimates obtained with GGA and GGA + U. For GaAs(c), however, while the bulk modulus is in very good agreement with experiments, the equilibrium lattice spacing is underestimated and the band gap significantly overestimated, worsening, for both quantities, the accuracy of the results obtained with GGA and GGA + U. Our results thus confirm that Ga 3d should be treated as valence states; in the present study, however, they are not directly subject to the Hubbard functional.

Despite the overall improvement obtained with GGA + U + V, some discrepancies with the experimental results still persist regarding, especially, the equilibrium lattice constant and the bulk modulus. However, it should be kept in mind that computational results presented in this section would be directly comparable to 0 K measurements, for which slightly shorter lattice parameters and slightly higher bulk moduli are predicted [82] (see the footnotes of table 3 for details).

Figure 4 displays the GGA and GGA + U + V band structures and density of states for Si and GaAs. The energies were shifted so that the top of the valence band corresponds to the zero of the energy in all cases. The correction introduced by the GGA + U + V (with respect to the GGA band structure) to the conduction band consists in an almost rigid upward shift in energy. In the valence manifold, however, the correction to the energy levels acquires a slight k-dependence and has a more pronounced effect on the lowest energy level, which is shifted downward. This latter effect results in an increase of the total bandwidth of these systems (by 0.6 eV for GaAs and by 0.8 eV for Si) compared to GGA, and accounts for perfect agreement with experimental results (the measured bandwidth is 12.5 eV for Si and 13.2 eV for GaAs [78]).

In summary, the GGA + U + V shows significant improvement over GGA and GGA + U in the description of the structural and electronic properties of Si and GaAs. Although the dominant effect arises from the interaction between nearest-neighbor sites, for both Si and GaAs the inclusion of the coupling between further neighbors could bring a refinement of the results presented in this section. Also, in the case of GaAs with Ga 3d electrons in valence, more accurate results could be obtained accounting for the hybridization of these states with 4s and 4p orbitals (probably the overlap with the states of As is quite limited) and including the corresponding interaction parameter in the '+U + V' corrective functional. Since the GGA and the GGA + U + V ground states are qualitatively similar, we expect a 'self-consistent' evaluation of U and V to have a minor effect on the presented results both for Si, and GaAs.

4. Conclusions

In this paper we have introduced a useful generalization of the popular DFT + U method that, modeled on the extended Hubbard Hamiltonian, includes on-site (U) and inter-site (V) electronic interactions and is able to correct up to two angular momentum manifolds per atom. The competition between the two kinds of electronic couplings avoids the over-stabilization of occupied atomic orbitals, often affecting the on-site DFT + U, and allows for the description of more general ground states where electrons 'localize' on hybridized (e.g., molecular) orbitals. The flexibility in the representation of occupied states is further enhanced by the larger number of orbital manifolds that are simultaneously subject to the action of the corrective functional. Numerical accuracy is guaranteed by the linear-response calculation of U and V that allows one to evaluate the relative strength of the two couplings and, thus, to precisely determine the degree of electronic localization of the ground state.

The effectiveness of the method is demonstrated in this paper by its successful application to the quite diverse test systems NiO (Mott/charge-transfer insulator), Si and GaAs

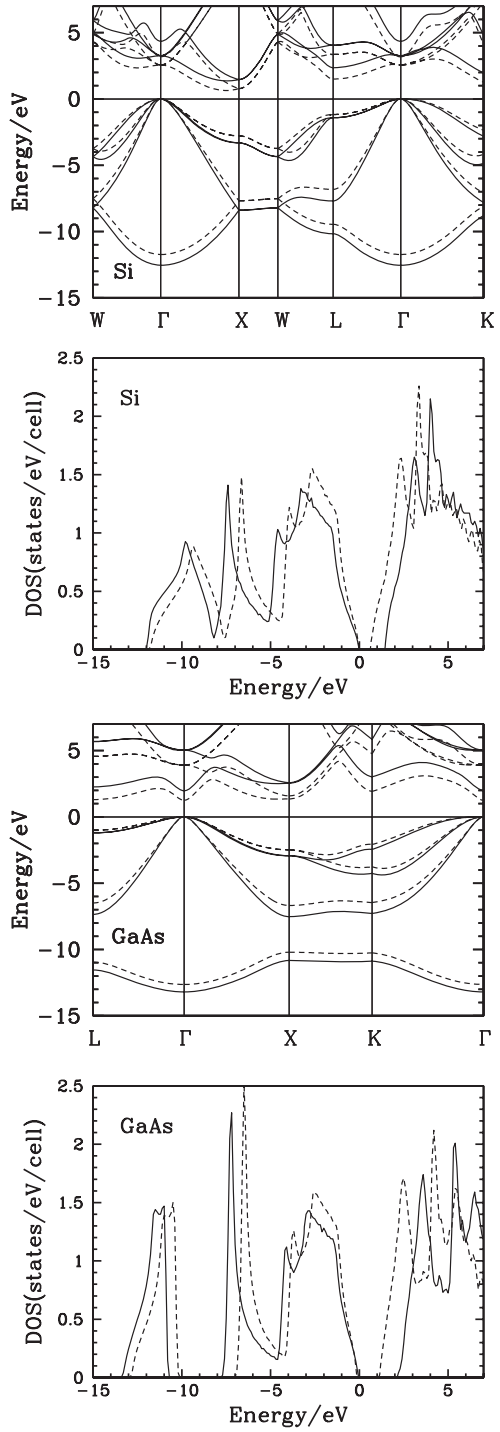

Figure 4. Band structure and density of states of Si and GaAs (core case). Continuous lines represent GGA + U + V results and dashed lines represent standard GGA results. All energies were shifted so that the top of valence bands are at zero energy.

(band semiconductors). For both classes of materials the use of the DFT + U + V functional results in a significant improvement (over approximate DFT and DFT + U) in the agreement of the structural (equilibrium lattice parameter and bulk modulus) and electronic (overlap of p and d states, band gap) properties with available experimental results. For Si and GaAs this improvement is more consistent, probably due to the higher level of structural isotropy of these materials, for which a corrective functional with orbital independent interactions is better suited.

The importance of these results is not limited to the more accurate description the selected test systems received. In fact, they demonstrate that the novel computational approach provides a unified theoretical framework able to treat systems, as diverse as Mott, charge-transfer, and band insulators, with equal accuracy and comparable computational effort. Furthermore, the use of the extended Hamiltonian provides a new route to improve the corrective functional in a systematic way, as it allows the addition of interactions between further shells of neighbors independently and, thus, to easily assess their individual contributions to the final results. This procedure also leads to the possibility to set calculations with minimal cost (with a minimal set of inter-site interaction terms).

Potential applications of this novel corrective functional are quite broad. Besides high T_c superconductors (for which the nearest-neighbor electronic couplings has sometimes been demonstrated to play a very important role), the remarkable success obtained with strongly localized (correlated) and strongly hybridized systems, suggests that intermediate situations where 'correlated' and 'non-correlated' orbitals show significant overlap (as, e.g., semiconductors doped with magnetic impurities, metallic active centers of molecular complexes, etc) and phenomena where a switch between different localization regimes is observed (e.g., in bond breaking and formation events) are likely to be described more accurately by the novel DFT+U+V scheme. This is especially true for isotropic systems that better fit the simple '+U + V' functional based on orbital independent interactions; more anisotropic materials may require, however, extra attention. The development of a more flexible corrective Hamiltonian based on orbital-dependent effective interactions, needed in these cases, is planned for future investigations.

Acknowledgments

MC thanks P M Grant, A Floris, E K U Gross and S de Gironcoli for very useful discussions. The authors are also grateful to the Minnesota Supercomputing Institute for providing computational resources and technical support that were essential for this work. Partial support from the NSF grant EAR-0810272 is gratefully acknowledged.

References

[1] Anisimov V I, Zaanen J and Andersen O K 1991 *Phys. Rev.* B **44** 943
[2] Anisimov V I, Aryasetiawan F and Liechtenstein A I 1997 *J. Phys.: Condens. Matter* **9** 767
[3] Hubbard J 1963 *Proc. R. Soc.* A **276** 238
[4] Hubbard J 1964 *Proc. R. Soc.* A **277** 237
[5] Hubbard J 1964 *Proc. R. Soc.* A **281** 401
[6] Hubbard J 1965 *Proc. R. Soc.* A **285** 542
[7] Hubbard J 1967 *Proc. R. Soc.* A **296** 82
[8] Hubbard J 1967 *Proc. R. Soc.* A **296** 100
[9] Austin I G and Mott N F 1970 *Science* **168** 71
[10] Anisimov V I, Poteryaev A I, Korotin M A, Anokhin A O and Kotliar G 1997 *J. Phys.: Condens. Matter* **9** 7359

[11] Liechtenstein A I and Katsnelson M I 1998 *Phys. Rev.* B **57** 6884
[12] Kobayashi S, Nohara Y, Yamamoto S and Fujiwara T 2008 *Phys. Rev.* B **78** 155112
[13] Jiang H, Gomez-Abal I, Rinke P and Scheffler M 2009 *Phys. Rev. Lett.* **102** 126403
[14] Anisimov V I, Elfimov I S, Hamada N and Terakura K 1996 *Phys. Rev.* B **54** 4387
[15] Anderson P W 1987 *Science* **235** 1196
[16] Anderson P W, Baskaran G, Zou Z and Hsu T 1987 *Phys. Rev. Lett.* **58** 2790
[17] Imada M 1991 *J. Phys. Soc. Japan* **60** 2740
[18] Hirsch J E, Loch E, Scalapino D J and Tang S 1988 *Physica* C **153–155** 549
[19] Thakur J S and Das M P 2007 *Int. J. Mod. Phys.* B **21** 2371
[20] Jursa R, Wermbter S and Czycholl G 1996 *Proc. of the 21st Int. Conf. on Low Temperature Physics* p 613
[21] Szabó Z and Gulácsi Z 1996 *Proc. of the 21st Int. Conf. on Low Temperature Physics* p 609
[22] de Mello E V L 1999 *Braz. J. Phys* **29** 551
[23] Mancini F, Mancini F P and Naddeo A 2009 *Eur. Phys. J.* B **68** 309
[24] Morohoshi S and Fukumoto Y 2008 *J. Phys. Soc. Japan* **77** 105005
[25] Watanabe T, Yokoyama H, Tanaka Y and Inoue J 2008 *J. Phys. Chem. Sol.* **69** 3372
[26] van Dongen P G J 1994 *Phys. Rev.* B **49** 7904
[27] Verdozzi C and Cini M 1995 *Phys. Rev.* B **51** 7412
[28] Zhu L Y and Wang W Z 2006 *J. Phys.: Condens. Matter* **18** 6273
[29] Carbone C *et al* 2009 arXiv:0907.2911 http://www.citebase.org/abstract?id=oai
[30] Dudarev S L, Botton G A, Savrasov S Y, Humphreys C J and Sutton A P 1998 *Phys. Rev.* B **57** 1505
[31] Liechtenstein A I, Anisimov V I and Zaanen J 1995 *Phys. Rev.* B **52** R5467
[32] Petukhov A G, Mazin I I, Chioncel L and Liechtenstein A I 2003 *Phys. Rev.* B **67** 153106
[33] Lechermann F, Fähnle M, Meyer B and Elsässer C 2004 *Phys. Rev.* B **69** 165116
[34] Cococcioni M and de Gironcoli S 2005 *Phys. Rev.* B **71** 35105
[35] Mazurenko V V, Skornyakov S L, Kozhevnikov A V, Mila F and Anisimov V I 2007 *Phys. Rev.* B **75** 224408
[36] Lechermann F, Georges A, Poteryaev A, Biermann S, Posternak M, Yamasaki A and Andersen O K 2006 *Phys. Rev.* B **74** 125120
[37] Miyake T and Aryasetiawan F 2008 *Phys. Rev.* B **77** 085122
[38] Marzari N and Vanderbilt D 1997 *Phys. Rev.* B **56** 12847
[39] Paudel T R and Lambrecht W R L 2008 *Phys. Rev.* B **78** 085214
[40] Kresse G, Gil A and Sautet P 2003 *Phys. Rev.* B **68** 073401
[41] Köhler L and Kresse G 2004 *Phys. Rev.* B **70** 165405
[42] Dabo I, Wieckowski A and Marzari N 2007 *J. Am. Chem. Soc.* **129** 11045
[43] Perdew J P and Levy M 1983 *Phys. Rev. Lett.* **51** 1884
[44] Lima N A, Oliveira L N and Capelle K 2002 *Europhys. Lett.* **60** 601
[45] Dreizler R M and Gross E K U 1990 *Density Functional Theory: An Approach to the Quantum Many-Body Problem* (Berlin: Springer)
[46] Godby R W, Schlüter M and Sham L J 1986 *Phys. Rev. Lett.* **56** 2415
[47] Grüning M, Marini A and Rubio A 2006 *J. Chem. Phys.* **124** 154108
[48] Sharma S, Dewhurst J K, Lathiotakis N N and Gross E K U 2008 *Phys. Rev.* B **78** R201103
[49] Giannozzi P *et al* 2009 *J. Phys.: Condens. Matter* **21** 395502 http://www.quantum-espresso.org
[50] Sawatzky G A and Allen J W 1984 *Phys. Rev. Lett.* **53** 2339
[51] Thuler M R, Benbow R L and Hurych Z 1983 *Phys. Rev.* B **27** 2082
[52] Fujimori A and Minami F 1984 *Phys. Rev.* B **30** 957
[53] Dudarev S L, Peng L-M, Savrasov S Y and Zuo J-M 2000 *Phys. Rev.* B **61** 2506
[54] Bengone O, Alouani M, Blöchl P and Hugel J 2000 *Phys. Rev.* B **62** 16392
[55] Rohrbach A, Hafner J and Kresse G 2004 *Phys. Rev.* B **69** 075413
[56] Gougoussis C, Calandra M, Seitsonen A, Brouder C, Shukla A and Mauri F 2009 *Phys. Rev.* B **79** 045118
[57] Moreira I P R, Illas F and Martin R 2002 *Phys. Rev.* B **65** 155102
[58] Feng X-B and Harrison N M 2004 *Phys. Rev.* B **69** 035114
[59] Ren X, Leonov I, Keller G, Kollar M, Nekrasov I and Vollhardt D 2006 *Phys. Rev.* B **74** 195114
[60] Kunes J, Anisimov V I, Skornyakov S L, Lukoyanov A V and Vollhardt D 2007 *Phys. Rev. Lett.* **99** 156404
[61] Miura O and Fujiwara T 2008 *Phys. Rev.* B **77** 195124
[62] Vanderbilt D 1990 *Phys. Rev.* B **41** 7892
[63] Perdew J P, Burke K and Ernzheroff M 1996 *Phys. Rev. Lett.* **77** 3865
[64] Monkhorst H J and Pack J D 1976 *Phys. Rev.* B **13** 5188
[65] Kulik H J, Cococcioni M, Scherlis D A and Marzari N 2006 *Phys. Rev. Lett.* **97** 103001
[66] Tsuchiya T, Wentzcovitch R M, da Silva C R S and de Gironcoli S 2006 *Phys. Rev. Lett.* **96** 198501
[67] Hsu H, Umemoto K, Cococcioni M and Wentzcovitch R M 2009 *Phys. Rev.* B **79** 125124
[68] *CRC Handbook of Chemistry and Physics* 1998 (Boca Raton, FL: CRC Press)
[69] Huang E, Jy K and Yu S-G 1994 *J. Geophys. Soc. China* **37** 7
[70] Nielsen O H and Martin R M 1985 *Phys. Rev.* B **32** 3792
[71] Filippi C, Singh D J and Umrigar C J 1994 *Phys. Rev.* B **50** 14947
[72] Juan Y-M, Kaxiras E and Gordon R C 1995 *Phys. Rev.* B **51** 9521
[73] Giannozzi P, de Gironcoli S, Pavone P and Baroni S 1991 *Phys. Rev.* B **43** 7231
[74] Lee I H and Martin R M 1997 *Phys. Rev.* B **56** 7197
[75] Städele M, Moukara M, Majewski J A, Vogl P and Görling A 1999 *Phys. Rev.* B **59** 10031
[76] Nguyen H-V and de Gironcoli S 2009 *Phys. Rev.* B **79** 205114
[77] Heyd J, Sucseria G E, Martin R L and Peralta J E 2005 *J. Chem. Phys.* **123** 174101
[78] Rohlfing M, Krüger P and Pollmann J 1993 *Phys. Rev.* B **48** 17791
[79] Aulbur W G, Jönsson L and Wilkins J W 1999 *Solid State Phys.* **54** 1
[80] Aulbur W G, Städele M and Görling A 2000 *Phys. Rev.* B **62** 7121
[81] von Lilienfeld O A and Schultz P A 2008 *Phys. Rev.* B **77** 115202
[82] http://www.ioffe.ru/SVA/NSM/Semicond/